Emission of particulate and gaseous pollutants from household laser processing machine

Hyun Sik Ko [1,2,3,**], Sang Bin Jeong [2,3,**], Sooyeol Phyo [2,4], Jiwon Lee [2], Jae Hee Jung [1,*]

[1] Department of Mechanical Engineering, Sejong University, Seoul 05006, Republic of Korea
[2] Center for Environment, Health, and Welfare Research, Korea Institute of Science and Technology (KIST), Seoul 02792, Republic of Korea
[3] Graduate School of Energy and Environment, Korea University, Seoul 02841, Republic of Korea
[4] Department of Materials Science and Engineering, Korea University, Seoul 02841, Republic of Korea

ARTICLE INFO

ABSTRACT

Indoor air quality (IAQ) directly affects the health of occupants. Household manufacturing equipment (HME) used for hobbies or educational purposes is a new and unexplored source of air pollution. In this study, we evaluated the characteristics of particulate and gaseous pollutants produced by a household laser processing equipment (HLPE). Various target materials were tested using a commercial HLPE under various operating conditions of laser power and sheath air flow rate. The mode diameters of the emitted particles gradually decreased as laser power increased, while the particle number concentration (PNC) and particle emission rate (PER) increased. In addition, as the sheath air flow rate quadrupled from 10 to 40 L/min, the mode diameter of the emitted particles decreased by nearly 25%, but the effect on the PNC was insignificant. When the laser induced the target materials at 53 mW, the mode diameters of particles were <150 nm, and PNCs were >2.0 × 10^4 particles/cm^3. Particularly, analyses of sampled aerosols indicated that harmful substances such as sulfur and barium were present in particles emitted from leather. The carcinogenic gaseous pollutants such as acrylonitrile, acetaldehyde, 1,3-butadiene, benzene, and C$_8$ aromatics (ethylbenzene) were emitted from all target materials. In an actual indoor environment, the PNC of inhalable ultrafine particles (UFPs) was >5 × 10^4 particles/cm^3 during 30 min of HLPE operation. Our results suggest that more meticulous control methods are needed, including the use of less harmful target materials along with filters or adsorbents that prevent emission of pollutants.

© 2020 The Research Center for Eco-Environmental Sciences, Chinese Academy of Sciences. Published by Elsevier B.V.

* Corresponding author.
  E-mail: jaehee@sejong.ac.kr (J.H. Jung).
** These authors contributed equally to this work.

Introduction

Recently, the popularity of creative, rather than commercial, activities has led to the development of do-it-yourself (DIY) culture. In response to this phenomenon, a variety of types of small-scale manufacturing equipment, such as NC-lathes, welders, 3D printers, and laser processors have become commercially available and widely used in home and office settings. Each piece of household manufacturing equipment (HME) comes with safety guidelines for its users, but these guidelines are not comprehensive. For example, HME can be a source of indoor air pollution.

There are major differences between the use of equipment in workplaces and in the home. In workplaces, the types and concentrations of pollutants generated from equipment operation are monitored for compliance with the relevant national and international regulations. Experts operate equipment with awareness of the expected pollutants and use protective devices (OSHA, 1993). However, most HME is operated with few protective measures. Because HME is generally smaller-scale versions of existing equipment, pollutant generation is reduced but not absent. Accordingly, studies have been conducted on the effects of HME, including 3D printers, laser printers, and welders, in indoor environments. For example, 3D printers, which differ according to the filament type, have been found to emit high concentrations of particulate and gaseous contaminants (Azimi et al., 2016; Kim et al., 2015). Laser printers also emit sub-micron particles at high concentrations (McGarry et al., 2011). In particular, welders emit hazardous fumes that can have fatally toxic effects on the respiratory tract (Antonini, 2003). HME is capable of producing aerosols and gas-phase pollutants that adversely affect the health of the user. Among the various types of HME, household laser processing equipment (HLPE) has recently become common in homes, offices, and schools. Laser processing operates on the principle of localized irradiation, using a laser beam focused on the surface of the target material to produce thermal effects, including laser ablation, welding, drilling, marking, and engraving (Kraus et al., 2017; Pashby et al., 2003). Laser processing is widely applied in a variety of manufacturing processes due to its high precision, convenience, and broad applicability. Laser processing must be conducted in a controlled environment because it inevitably produces various detrimental byproducts such as fumes, airborne fine particles and volatile organic compounds (VOCs) (Vassie et al., 1995; Nimmrichter et al., 2007; Walter et al., 2014). Even at the relatively small scale of HLPE, considerable levels of harmful substances can be generated.

Numerous studies have indicated that exposure to airborne fine particles has a strong relationship with various diseases, aggravating asthma, strokes, cardiovascular disorders and respiratory diseases and even causing premature death (Brook et al., 2010; Delfino et al., 2006; Kettunen et al., 2007). In an effort to manage fine particles, the Environmental Protection Agency (EPA) regulates particles in two representative categories according to their predicted penetration capacity into the lung, known as PM_{10} and $PM_{2.5}$ (particulate matter with an aerodynamic diameter of ≤ 10 and ≤ 2.5 µm, respectively) (USEPA, 2017). In particular, $PM_{2.5}$ is classified as a Group 1 carcinogen by the International Agency for Research on Cancer (IARC) of the World Health Organization (WHO) (IARC, 2012a; Loomis et al., 2013). In addition to fine particles, VOCs can also have various acute and chronic health effects. Many VOCs are classified as possible human carcinogens or toxicants, which may cause neurological symptoms such as headache, as well as nausea, and asthma (Bernstein et al., 2008; Lehmann et al., 2001; Levy et al., 2019). However, most HLPE do not have mechanisms to prevent hazardous substance production, such as air filtration or ventilation. In addition, users at home or school generally do not use personal protective equipment and may awareness about harmful substances in the air. Therefore, it is important to evaluate the physicochemical properties of the pollutants emitted from HLPE to prevent potential exposure and the associated risks to users.

In this study, we evaluated the characteristics of aerosols and VOCs emitted during the operation of commercial HLPE using various target materials and operating conditions such as laser power and sheath air flow rate. The size distribution and concentration of the particles emitted were analyzed in real time, and the characteristics of VOCs were evaluated using a proton-transfer-reaction time-of-flight mass spectrometer (PTR-ToF-MS). In addition, variation in particle concentration was observed in an actual indoor environment.

1. Materials and methods

1.1. HLPE and air pollutant measurement

Commercially available HLPE was used for the experiment. The size of the HLPE was 152 mm × 142 mm × 190 mm and had a power of 1.5 W, a 405 nm wavelength laser module, and a two-axis translation stage allowing for an engraving space of 42 mm × 42 mm. The HLPE was placed in an acryl housing with a sheath air inlet and outlet to accurately measure the emitted particulate and gaseous contaminants. During laser irradiation, clean sheath air, which was filtered through a high-efficiency particulate air (HEPA) filter, was supplied using a mass flow controller (MFC; FC-280S, Mykrolis Corp., MA, USA). Then, the emitted contaminants were carried to the outlet of the device housing. Various target materials (wood, rubber, cork, and leather) were loaded on top of the transfer stage module based on the focal length of the laser beam.

A schematic diagram of the experimental setup used to measure emitted particulate and gaseous contaminants is shown in Fig. 1. The induced laser power was controlled using a power supply (MK-3003D, MK POWER, Seoul, Republic of Korea), and the two-axis translation stage was aided by laser irradiation of the desired surface of the target material. Simultaneously, the emitted contaminants were transported to the outlet with the sheath air. The size distribution and concentration of the particulate contaminants were measured using a fast mobility particle sizer (FMPS, model 3091, TSI Inc., USA) with a detection range of 5.6 to 560 nm. The particle emission rate (PER) was calculated as follows:
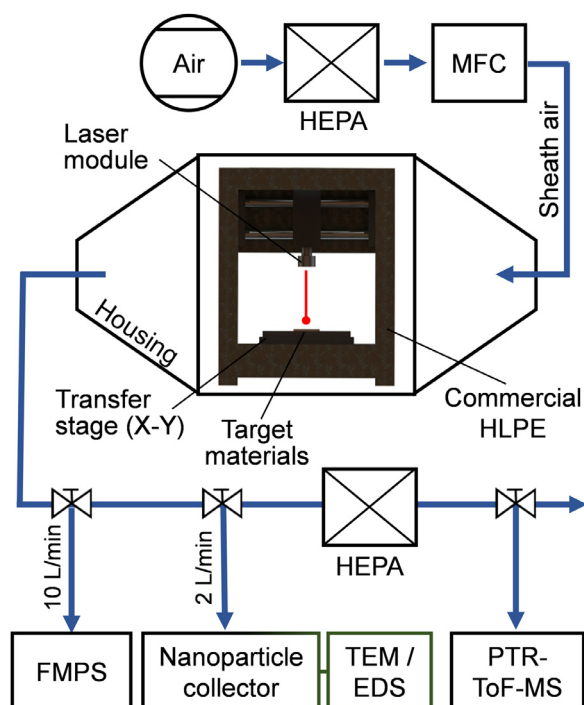
$$PER = N \times V_{flow} \tag{1}$$

Fig. 1 – Schematic diagram of the experimental setup used to measure emitted pollutants from household laser processing equipment (HLPE). The sheath air through a high efficiency particulate air (HEPA) filter is controlled by a mass flow controller (MFC). The particulate and gaseous pollutants were quantified using a fast mobility particle sizer (FMPS) and a proton-transfer-reaction time-of-flight mass spectrometry (PTR-ToF-MS), respectively. The morphology and chemical composition of the particles were ananlyzed through a transmission electron microscopy (TEM) and an energy-dispersive X-ray spectroscopy (EDS), respectively.

where N (particles/cm^3) is the particle number concentration (PNC) and V_{flow} (L/min) is the flow rate at the air outlet. After measurement, the inside of the housing was fully washed with clean air for at least 1 hr.

To examine the morphology and the chemical composition of the emitted particles, a nanoparticle collector (HCT 4650, HCT Co., Republic of Korea) was used. Emitted particles were collected on the surface of a copper-grid (CF-300U, Electron Microscopy Sciences, USA) in the nanoparticle collector for 10 min at a flow rate of 2 L/min. The morphology and chemical composition of the collected particles were analyzed using transmission electron microscopy (TEM; Titan F20G, FEI, Hillsboro, USA) and energy-dispersive X-ray spectroscopy (EDS), respectively.

The emitted gases including VOCs were measured using proton transfer reaction time-of-flight mass spectrometry (PTR–ToF–MS; Vocus PTR-ToF 2R, Aerodyne Research Inc., USA) with a flow rate of 0.1 L/min. The data reported in this study included 40–150 of mass-to-charge ratio (m/z) VOCs, which comprised 98% of the total measured VOCs. ToF data were analyzed using the Tofware software package (Aerodyne Research

Inc.), and the raw data were corrected for duty cycle discrimination in the ToF extraction region (Fig. S1).

1.2.   Laser irradiation conditions

The physical and chemical properties of the emitted particles were evaluated under various laser power and sheath air flow rate conditions. First, testing was carried out under various laser power conditions. The intrinsic laser power of commercial HLPE (47, 52, and 102 mW) used for the test. The sheath air flow rate was fixed at 10 L/min, a wood board (30 mm × 100 mm × 3 mm) was used as the target material. Second, the effects of sheath air on particle characteristics were investigated. The laser power was set to 102 mW and three different air flow rates were selected (10, 25, and 40 L/min) for irradiation on the wood board. The flow rate of sheath air was controlled using the MFC. Subsequently, the characteristics of the particles and gases emitted from the target material were investigated. Rubber, cork, and leather samples were trimmed to the same size and tested. Materials that are easily accessible and widely used at home and school for making or engraving using laser processing equipment were selected. The laser power, irradiation area, and sheath air flow rate were fixed at 53 mW, 4.6 cm^2, and 10 L/min, respectively. In all tests, laser irradiated was conducted for 1 hr at 0.063 sec/spot. All experiments were conducted in triplicate.

1.3.   Indoor test

An indoor test of the HLPE was conducted in a naturally ventilated office with a volume of approximately 32 m^3 (Fig. S2). To avoid effects from external airflow, all ventilation systems were switched off and all windows and doors were closed. No major sources of particulate or gaseous pollutants were present. The HLPE was placed on a desk (height, 0.8 m) and the concentrations of emitted particles were measured using an FMPS installed at a distance of 1 m from the device at a height of 1 m. Laser irradiation of the wood board was carried out with a laser power of 102 mW and an irradiation time of 0.063 sec/spot. The indoor test was conducted in three steps: 1 hr of pre-operation (background measurement, HLPE off), 1 hr of HLPE operation (HLPE on), and 1 hr of post-operation (HLPE off). The room was cleaned using a ventilation system at five air exchanges per hour for about 2 hr to insure that the emitted particles were removed.

2.   Results and discussion

2.1.   Characteristics of particles emitted under various laser power conditions

The physical characteristics of particles emitted from the wood board were evaluated under constant sheath air flow of 10 L/min and various laser power conditions. Fig. 2a shows a contour plot illustrating temporal variation in the particle size distribution. At a laser power of 102 mW, particles were stably emitted during operation and exhibited a unimodal size curve with a mode (peak) diameter of 124 ± 0.01 nm. The PNC also remained at a nearly constant level (˜1.5 × 10^5 particles/cm^3)
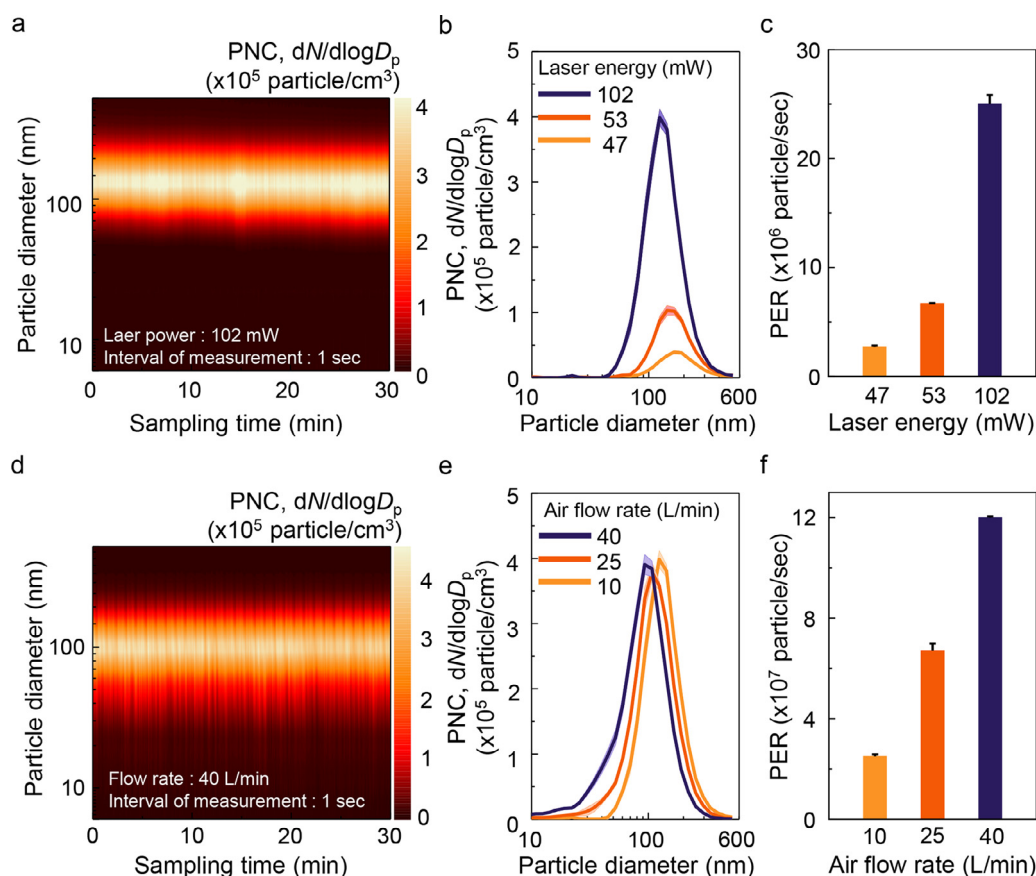
Fig. 2 – Characteristics of particles emitted from a wood board under various induced laser power conditions and sheath air flow rate (irradiation time: 0.063 sec/spot). (a) 2D contour graph of particles emitted over 30 min, (b) size distribution and normalized particle number concentration (PNC) of emitted particles, and (c) particle emission rate (PER) versus laser power with a sheath air flow rate 10 L/min ($n = 3$). Normalized concentration ($dN/dlogD_p$) is used to describe PNC, where dN is the number of particles in the range and $dlogD_p$ is the difference in the log of the channel width. (d) 2D contour graph of particles emitted over 30 min, (e) size distribution and normalized PNC of emitted particles, and (f) PER versus air flow rate with the laser power 102 mW ($n = 3$). Error bars indicate standard deviation.

for 30 min. After ensuring the stability of the device, measurement was conducted under various laser power conditions. The size distributions of emitted particles are shown in Fig. 2b. When the laser power decreased from 102 to 47 mW, the PNC decreased ($(1.5 \pm 0.05) \times 10^5$ to $(0.16 \pm 0.08) \times 10^5$ particles/cm^3), and the mode diameter tended to increase (124.1 ± 0.01 to 165.5 ± 0.01 nm). Variation in the geometric standard deviation (GSD) of particles was insignificant. As the PNC changed, the PER decreased from $(25.1 \pm 0.83) \times 10^6$ to $(2.7 \pm 0.13) \times 10^6$ particles/sec (Fig. 2c). Details of the physical characteristics of particles, including induced laser power, mode diameter, geometric mean diameter (GMD), GSD, PNC, and PER are presented in Table S2.

In HLPE, particle generation is related to the behavior of laser-induced plasma. Particles can be generated during plasma cooling through aerosol condensation and collisions between vaporized atoms and molecules in the plasma (Gu et al., 2015). Laser power increases the surface temperature of the target material as well as the internal energy. In turn, the enhanced internal energy enables more efficient physical separation of the components of the target material,

enhancing conditions for vapor formation (Brailovsky et al., 1995). In addition, as more laser power is applied, it is increasingly absorbed by the vapor to form more plasma. Therefore, PNC inevitably increases with increasing induced laser energy (Kawakami et al., 1999; Ullmann et al., 2002). Meanwhile, the mode diameter of the particles emitted decreased slightly as their induced laser power increased. Under the condition of standard pressure, increased laser-induced thermal energy leads to higher heat conduction and higher diffusivity, resulting in faster cooling of the vapor plume. This increased cooling rate reduces collisions between plasma components (Hergenröder, 2006; Zhang et al., 2014). Therefore, the GSD remained almost constant, but relatively smaller particles were emitted with higher laser-induced power.

2.2. Characteristics of particles emitted under various air flow rate conditions

The physical characteristics of laser-induced particles were evaluated under constant laser power of 102 mW and various air flow rate conditions. The laser power and irradiation time
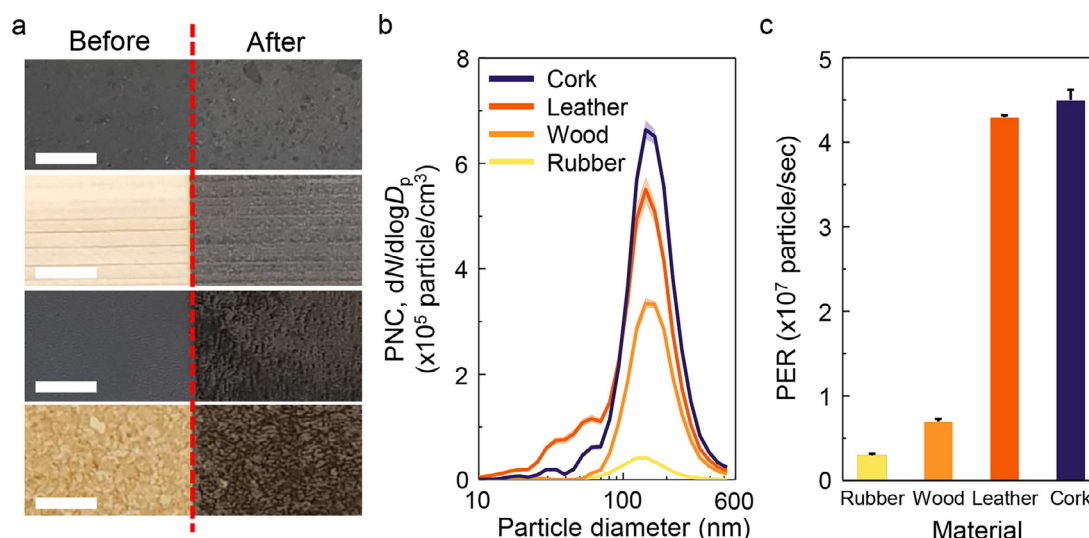
Fig. 3 – Characteristics of particles emitted from various target materials (laser power 53 mW, sheath air flow rate 10 L/min, irradiation time 0.063 sec/spot). (a) Images of target materials before and after laser processing. Scale bars represent 5 mm. (b) Size distribution and concentration of emitted particles. (c) PER for various target materials. Error bars indicate standard deviation ($n = 3$).

Table 1 – Physical characteristics of particles emitted from various target materials (laser power 53 mW, sheath air flow rate 10 L/min, irradiation time 0.063 sec/spot).

Material	Mode diameter (nm)	GMD (nm)	GSD	PNC ($\times 10^5$ particles/cm^3)	PER ($\times 10^7$ particles/sec)
Rubber	143.0 ± 2.48	136.3 ± 1.13	1.5 ± 0.01	0.2 ± 0.01	0.3 ± 0.02
Wood	150.2 ± 10.87	158.6 ± 2.31	1.5 ± 0.04	0.4 ± 0.02	0.7 ± 0.03
Leather	143.3 ± 0.01	121.7 ± 2.58	1.9 ± 0.06	2.6 ± 0.01	4.3 ± 0.02
Cork	145.9 ± 7.18	149.9 ± 2.66	1.6 ± 0.05	2.7 ± 0.07	4.5 ± 0.12

GMD: geometric mean diameter; GSD: geometric standard deviation.

were fixed at 102 mW and 0.063 sec/spot, respectively. Particles were stably emitted even at a high flow rate of 40 L/min, with a mode diameter of 93.5 ± 2.63 nm, GSD of 1.7 ± 0.02, and PNC of $(1.8 \pm 0.08) \times 10^5$ particles/cm^3 over 30 min (Fig. 2d). The characteristics of particles varied during continued reduction of the sheath air flow rate from 40 to 10 L/min, as shown in Fig. 2e. As the air flow rate decreased, the mode diameter increased to 124.1 ± 0.01 nm, while the PNC was reduced slightly to $(1.5 \pm 0.05) \times 10^5$ particles/cm^3 (Table S3). As the particle concentration and sheath air flow rate decreased, the PER was reduced from $(1.2 \pm 0.05) \times 10^8$ to $(2.5 \pm 0.08) \times 10^7$ particles/sec (Fig. 2f).

As the sheath air flow rate decreased, the mode diameter tended to increase due to increased probability of collisions between plasma vapor components (Gaertner and Lydtin, 1994). The PNC was expected to decrease due to the cooling effects of high air flow rates, but the variation in PNC during measurement was insignificant. Because PER is proportional to the sheath air flow rate, it was predicted to reach lower values as the air flow decreased. Based on the results, sheath air flow rate had little effect on PNC, but caused notable changes in PER. It can also be inferred from the PER that the total number of particles generated is proportional to the operating time of HLPE.

2.3. Characteristics of particles emitted from various target materials

Various target materials (wood, rubber, cork, and leather) were used for measurement. Fig. 3a shows the materials before and after laser processing, showing changes to the surfaces of the target materials. Each target material was processed for 1 hr with constant laser irradiation, and the surfaces of all materials were blackened. The size distribution of particles emitted from each target material is illustrated in Fig. 3b. The mode diameter of particles emitted from wood was largest (151.8 ± 10.87 nm), and that from rubber was smallest (143.0 ± 2.48 nm). However, the difference in all mode diameters was less than 10 nm, and was insignificant (Table 1). The target material with the most irregular particle size distribution, which showed the highest GSD (1.9 ± 0.06), was leather. Among the physical characteristics observed, PNC showed a distinct difference. High PNC values were measured from cork and leather ($2.7 \pm 0.07) \times 10^5$ and $(2.6 \pm 0.01) \times 10^5$ particles/cm^3, respectively); accordingly, PER was also high in these two target materials (Fig. 3c).

TEM images of particles emitted from each material are shown in Fig. 4a. The particles arising from laser irradiation were irregular in shape and variable in size. The
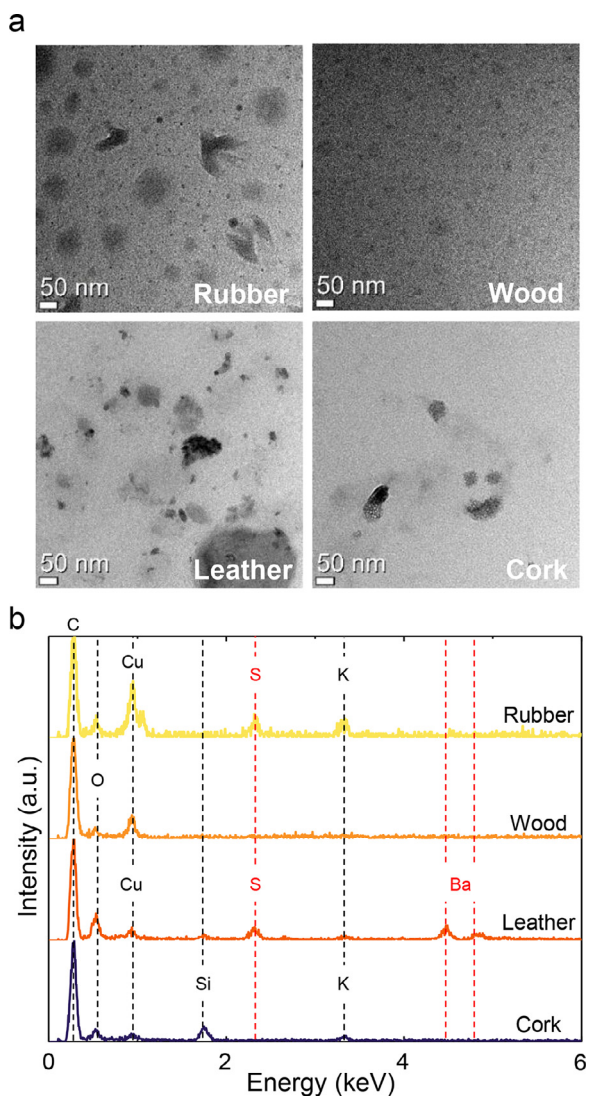
a

b

Fig. 4 – (a) Transmission electron microscopy (TEM) images and (b) energy-dispersive X-ray spectroscopy (EDS) analyses results of particles emitted from each target material. Experimental conditions: laser power 53 mW, sheath air flow rate 10 L/min, and irradiation time 0.063 sec/spot.

chemical composition of the particles was analyzed through EDS (Fig. 4b). The laser-generated particles were found to all have high carbon and oxygen contents. Because of the copper-TEM-grid used in the nanoparticle collector, copper was also detected in all analyses. Potassium was detected in all particles except those from wood, and sulfur was observed in those from rubber and leather. In addition, barium was found in leather particles.

We confirmed experimentally that the properties of the emitted particles could vary among target materials, even under the same laser irradiation condition. The roughness of the surface, color-dependent effects on absorbance, and the bond strength between the components of each material may have determined the particle characteristics. Most importantly, laser processing created UFPs emissions regardless of material. In addition, according to EDS results, the UFPs emit-

ted may have adverse health effects not only through physical, but also chemical mechanisms. If particles containing sulfur penetrate the body, they may lead to bronchoconstriction, elevated blood pressure and anemia (Komarnisky et al., 2003), while barium is a heavy metal linked to asthma (Kravchenko et al., 2014). Not only sulfur and barium, but also various other harmful chemical elements, may be present in the particles produced from various target materials. Therefore, HLPE should be used in a location and manner that minimizes the potential for adverse effects on users' health.

2.4. Characteristics of VOCs from various target materials

Table S4 summarizes the emission rates of the most abundant and hazardous VOCs among 70 VOCs (40–150 m/z) emitted from materials and measured using PTR-ToF-MS. The VOCs were monitored before and after the laser irradiation for 30 min. The concentrations of each component were averaged beginning at 5 to 10 min of laser irradiation (0 min), when the intensity plateaued. The five most abundant VOCs from each material are listed in order of their emission rates in Table S4. In addition, sixteen non-carcinogenic and five carcinogenic VOCs were selected based on their reference concentration for inhalation exposure (RfC) and inhalation unit risk, respectively (USEPA, 2020). The five top VOCs made up half (50%–55%) of the total emission rate and were mostly oxygenated VOCs including functional groups such as aldehyde, ketone, carboxylic acid, and ether with saturated or unsaturated carbons, which were created through thermal decomposition induced by laser irradiation.

The highest total emission rate of VOCs was observed from wood (327.68 ng/sec), as the laser power was sufficient to generate gas molecules from the cellulose or lignin of the wood. Cork emitted the second highest level of VOCs (302.47 ng/sec) for a similar reason. The VOCs emitted from wood and cork were similar, including acetaldehyde, acrolein, acetone, acetic acid, and methyl acetate. These compounds primarily arise from the oxidation or thermal decomposition of terpenoids, isoprene, or cellulose (McDonald et al., 2000). However, the concentrations of some of the most abundant VOCs (1,3-butadiene and methyl vinyl ketone) differed between these two materials due to their compositions or surface treatments. The emission rate from leather was 266.97 ng/sec and that from rubber was 32.71 ng/sec, which was only 10% of the emission rates from wood and cork. The reason for these large differences is likely that rubber consists of high-molecular-weight polymers of organic compounds, which the laser power was insufficient to decompose.

Fig. 5 shows a comparison of the emission rates of selected VOCs used for cancer and non-cancer risk assessments. During the process, all materials emitted considerable amounts of carcinogens such as acrylonitrile, acetaldehyde, 1,3-butadiene, benzene, and C_8 aromatic (ethylbenzene) substances. Those compounds are classified in IARC Group 1 (benzene, 1,3-butadiene), Group 2A (acetaldehyde), or Group 2B (acrylonitrile, ethylbenzene) (IARC, 1999). While rubber emitted a low level of carcinogens (1.63 ng/sec), cork released a high level (53.89 ng/sec), followed by leather (40.43 ng/sec) and wood (26.29 ng/sec). Although these concentrations are
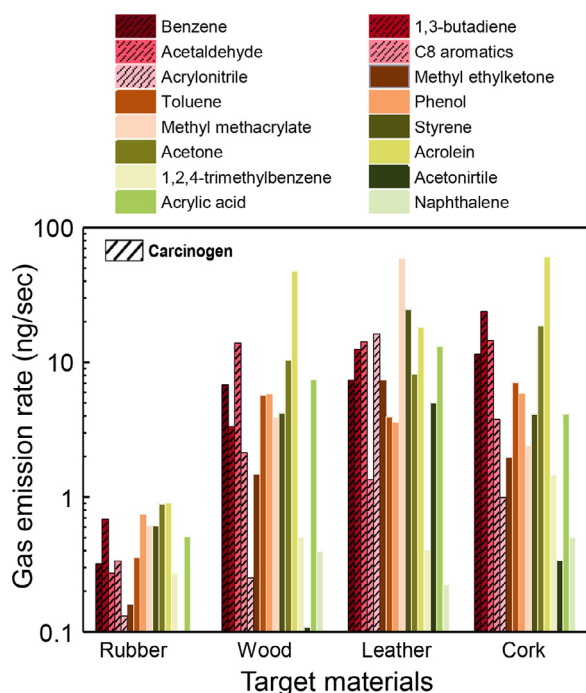
Fig. 5 – Volatile organic compound (VOC) emission rate from each target material measured using proton-transfer-reaction time-of-flight mass spectrometry (PTR-ToF-MS). Hatching indicates carcinogenic substances. Experimental conditions: laser power 53 mW, sheath air flow rate 10 L/min, and irradiation time 0.063 sec/spot.
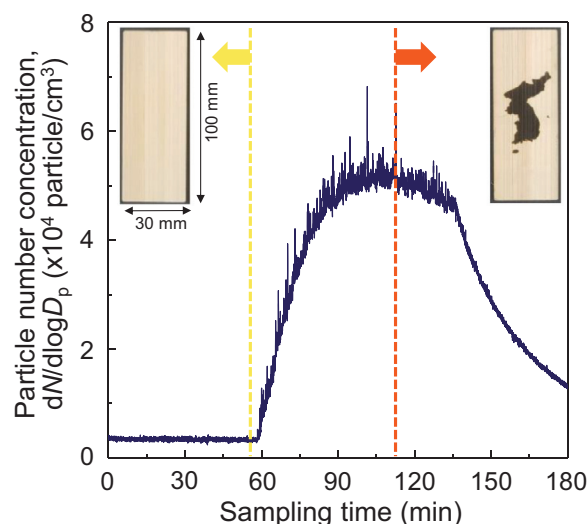

Fig. 6 – Variation in particle number concentration during the indoor measurement test of HLPE (household laser processing equipment) operation. The laser-induced area in the shape of the Korean peninsula is 3.32 cm^2.

below permissible exposure limits (note that permissible exposure limits apply only to workers), the most abundantly emitted carcinogens, such as acetaldehyde and 1,3-butadiene, also cause irritation of the eyes, nose, and throat and neurological and dermatological effects at very high levels of exposure (IARC, 2012b, 2019; OSHA, 1998). With regard to non-carcinogens, Fig. 5 compares the release of sixteen compounds, showing that each material released very different levels of various compounds. The total levels of non-carcinogens emitted from leather, wood, cork, and rubber were 187.78, 107.388, 105.069, and 6.547 ng/sec, corresponding to 70.3%, 32%, 49.7%, and 20% of the total VOCs, respectively. The emission rates of acrolein were highest from wood, cork, and rubber, whereas the most methyl methacrylate was released from leather. Those compounds can irritate the skin, eyes, and nose and have chronic effects. In addition, the minimal risk levels (MRLs) of acrolein are 3 ppbV for acute duration (1–14 days) and 0.4 ppbV for intermediate duration (15–364 days), as established by the Agency for Toxic Substances and Disease Registry (ATSDR) (ATSDR, 2007). The measured concentrations of acrolein (67.02, 176.06, 225.51, and 3.33 ppbV) released from leather, wood, cork, and rubber well exceeded their MRLs, indicating that long-term exposure without personal protective equipment (PPE) may harm health.

2.5.   Indoor measurement during operation of HLPE

Fig. 6 shows the results of laser irradiation of a wood board in the shape of the Korean peninsula in a real indoor environ-

ment. The time and area of laser irradiation were 60 min and 3.32 cm^2, respectively. The PNC increased steadily for 30 min after HLPE operation began, and tended to become saturated at high concentrations ($>5 \times 10^4$ particles/cm^3). After operation was stopped (at 120 min), the PNC gradually decreased. Compared to the previous housed HLPE experiment, relatively low PNC values were measured due to the lack of sheath air flow, which allowed the emitted particles spread to various directions rather than being carried in one direction. Nevertheless, UFPs were emitted at a considerable concentration.

In a similar fashion to HLPE, the typical HME used for hobby or educational purposes is the three-dimensional (3D) printer. The concentrations and emission rates of particles emitted from 3D printers were evaluated in a test chamber, and those for acrylonitrile butadiene styrene (ABS), a representative 3D printer filament, were found to exceed 9×10^5 particles/cm^3 and 1.0×10^{11} particles/min, respectively, (Azimi et al., 2016). A similar ABS has been reported to produce a particle concentration exceeding 1.5×10^5 particles/cm^3 (Kim et al., 2015). A binder jetting 3D printer using powder and binders has been reported to generate $>4 \times 10^5$ particles/cm^3 particles with diameters < 200 nm (Afshar-Mohajer et al., 2015). Thus, compared with previous HME particle emission results, HLPE also emits high concentrations of particulate pollutants. Although the measuring space, equipment, principle of particle generation, and chemical compositions differ among devices, most studies agree that HME can be a source of UFP emissions at considerable concentrations.

When HLPE is operated in indoor spaces, the possibility of UFPs reaching the human respiratory tract increases dramatically. UFPs can pass directly through the pulmonary blood-gas barrier, which consists of a monolayer of epithelial cells in the alveoli (Thorley et al., 2014). In addition, UFPs have a greater number concentration and a larger reactive surface area, where condensation or adsorption can occur, compared

to an equal mass of larger particles. The high reactive surface area can lead to significant adverse effects from interactions with cell membranes, protein structures, and other biological molecules that make up the human body (Chen et al., 2016). Therefore, users and suppliers of HME must be mindful of the serious health hazards of UFPs.

The indoor source emission rate is determined by the amount of emitted pollutants and ventilation rate per space volume. The most effective ways to minimize indoor exposure are to reduce equipment operating time and provide sufficient ventilation (Cooper and Alley, 2010). In particular, minimizing laser irradiation time can reduce the generation of contaminants. By adding an air filtration system or housing to the HLPE, the spread of particulate contaminants can be mitigated. In confined spaces, pollutant concentrations increase rapidly; therefore, equipment should be operated only in spaces with sufficient ventilation.

In addition, the selection of target material should be considered for HLPE use. The emission rates of gaseous and particulate pollutants were not proportional, and their components were markedly different. In particular, it was difficult to determine the chemical makeup of the leather sample, but given that sulfur, barium and relatively high levels of carcinogenic VOCs were detected, chemical treatment was likely used during the manufacture of the product. While we do not suggest that certain materials are safe for indoor HLPE operation, we recommend the use of materials with little or no chemical treatment.

For future research, the limitations of this study should be addressed. First, only four target materials were tested for particle and VOC generation. As the byproducts and type of chemical compound on the particles, such as semi-VOCs (SVOCs), vary with the properties of the target material, further research is needed to predict the levels of the various pollutants generated (McDonald, 2000; Kim, 2016). Second, only engraving HLPE was used among numerous types of HLPE. Although engraving HLPE is widely distributed, the amount and intensity of pollutants may differ with among HLPE types due to differences in intensity and method. Finally, evaluation of the ventilation effects in the actual indoor experiment was limited. In addition,

3. Conclusions

We confirmed that the concentrations of airborne particles and VOCs increased during HLPE operation. The physicochemical characteristics of particles varied depending on the target material and surrounding conditions, including laser power and sheath air flow rate. UFPs were generated at high concentrations proportional to laser power, regardless of the target material. Carcinogenic VOCs including acrylonitrile, acetaldehyde, benzene, and C_8 aromatic compounds were emitted. Therefore, HLPE can act as a source of indoor air pollutants and may cause disease through exposure to such pollutants.

Currently, most representative HME are 3D printers, laser printers, and welders. However, various types of HME including HLPE are now rapidly spreading to households and schools with limited environmental and sfaety restrictions. Our results indicate that more research into the use of HME

is needed, including the identification of less harmful substances and pollutant-blocking air filters or gas adsorbents, to protect the health vulnerable groups, such as children. In addition, it is essential to obtain the information necessary to establish standards or legislation that will minimize exposure to pollutants emitted from HME.

Declaration of competing interest

None.

Appendix A. Supplementary data

Supplementary material associated with this article can be found in the online version at doi:10.1016/j.jes.2020.10.018.

REFERENCES

Afshar-Mohajer, N., Wu, C-Y., Ladun, T., Rajon, D.A., Huang, Y., 2015. Characterization of particulate matters and total VOC emissions from a binder jetting 3D printer. Build. Environ. 93, 293–301.

Antonini, J.M., 2003. Health effects of welding. Crit. Rev. Toxicol. 33, 61–103.

ATSDR (Agency for Toxic Substances and Disease Registry), 2007. Medical Management Guidelines, Minimal Risk Levels (MRLs) – For Professionals. Available: https://www.atsdr.cdc.gov/mrls/mrllist.asp. Accessed September 28, 2020.

Azimi, P., Zhao, D., Pouzet, C., Crain, N.E., Stephens, B., 2016. Emissions of ultrafine particles and volatile organic compounds from commercially available desktop three-dimensional printers with multiple filaments. Environ. Sci. Technol. 50, 1260–1268.

Bernstein, J.A., Alexis, N., Bacchus, H., Bernstein, I.L., Fritz, P., Horner, E., et al., 2008. The health effects of nonindustrial indoor air pollution. J. Allergy Clin. Immunol. 121, 585–591.

Brailovsky, A.B., Gaponov, S.V., Luchin, V.I., 1995. Mechanisums of melt droplets and solid-particle ejection from a target surface by pulsed laser action. Appl. Phys. A 61, 81–86.

Brook, R.D., Rajagopalan, S., Pope III, C.A., Brook, J.R., Bhatnagar, A., Diez-Roux, A.V., et al., 2010. Particulate matter air pollution and cardiovascular disease: an update to the scientific statement from the American Heart Association. Circulation 121, 2331–2378.

Chen, R., Hu, B., Liu, Y., Xu, J., Yang, G., Xu, D., et al., 2016. Beyond PM$_{2.5}$: the role of ultrafine particles on adverse health effects of air pollution. BBA-Gen. Subjects 1860, 2844–2855.

Cooper, C.D., Alley, F.C., 2010. Air pollution control: A design approach. Waveland Press.

Delfino, R.J., Staimer, N., Gillen, D., Tjoa, T., Sioutas, C., Fung, K., et al., 2006. Personal and ambient air pollution is associated with increased exhaled nitric oxide in children with asthma. Environ. Health Perspect. 114, 1736–1743.

Gaertner, G., Lydtin, H., 1994. Review of ultrafine particle generation by laser ablation from solid targets in gas flows. Nanostruct. Mater. 4, 559–568.

Gu, D., Sun, Z., Medwell, P., Alwahabi, Z., Dally, B., Nathan, G., 2015. Mechanism for laser-induced fluorescence signal generation in a nanoparticle-seeded flow for planar flame thermometry. Appl. Phys. B-Lasers. O. 118, 209–218.

Hergenröder, R., 2006. Laser-generated aerosols in laser ablation for inductively coupled plasma spectrometry. Spectrochim. Acta B 61, 284–300.

IARC (International Agency for Research on Cancer), 1999. Acetaldehyde (Group 2B), Available: http://www.inchem.org/documents/iarc/vol71/005-acetaldehyde.html. Accessed September 28, 2020.

IARC (International Agency for Reasearch on Cancer), 2012a. Arsenic, Metals, Fibres, and Dusts, Available: http://monographs.iarc.fr/ENG/Monographs/vol100C/. Accessed September 28, 2020.

IARC (International Agency for Reasearch on Cancer), 2019. Agents Classified by the IARC Monographs, Volumes 1-125, Available: https://dtsc.ca.gov/wp-content/uploads/sites/31/2019/05/1-J-IARC-carcin.pdf. Accessed September 28, 2020.

IARC (International Agency for Reasearch on Cancer), 2012b. Chemical Agents and Related Occupations, Available: http://monographs.iarc.fr/ENG/Monographs/vol100F/. Accessed September 28, 2020.

Kawakami, Y., Seto, T., Ozawa, E., 1999. Characteristics of ultrafine tungsten particles produced by Nd: YAG laser irradiation. Appl. Phys. A-Mater. 69, S249–S252.

Kettunen, J., Lanki, T., Tiittanen, P., Aalto, P.P., Koskentalo, T., Kulmala, M., et al., 2007. Associations of fine and ultrafine particulate air pollution with stroke mortality in an area of low air pollution levels. Stroke 38, 918–922.

Kim, Y., Yoon, C., Ham, S., Park, J., Kim, S., Kwon, O., et al., 2015. Emissions of nanoparticles and gaseous material from 3D printer operation. Environ. Sci. Technol. 49, 12044–12053.

Kim, Y., Sartelet, K., Seigneur, C., Charron, A., Besombes, J.L., Jaffrezo, J.L., et al., 2016. Effect of measurement protocol on organic aerosol measurements of exhaust emissions from gasoline and diesel vehicles. Atmos. Environ. 140, 176–187.

Komarnisky, L.A., Christopherson, R.J., Basu, T.K., 2003. Sulfur: its clinical and toxicologic aspects. Nutr. 19, 54–61.

Kraus, E., Baudrit, B., Heidemeyer, P., Bastian, M., Stoyanov, O., Starostina, I., 2017. Surface treatment with ultraviolet laser for adhesive bonding of polymeric materials. J. Adhes. 93, 204–215.

Kravchenko, J., Darrah, T.H., Miller, R.K., Lyerly, H.K., Vengosh, A., 2014. A review of the health impacts of barium from natural and anthropogenic exposure. Environ. Geochem. Health 36, 797–814.

Lehmann, I., Rehwagen, M., Diez, U., Seiffart, A., Rolle-Kampczyk, U., Richter, M., et al., 2001. Enhanced in vivo IgE production and T cell polarization toward the type 2 phenotype in association with indoor exposure to VOC: results of the LARS study. Int. J. Hyg. Environ. Health 204, 211–221.

Levy, J., Neukirch, C., Larfi, I., Demoly, P., Thabut, G., 2019. Tolerance to exposure to essential oils exposure in patients with allergic asthma. J. Asthma 56, 853–860.

Loomis, D., Grosse, Y., Lauby-Secretan, B., El Ghissassi, F., Bouvard, V., Benbrahim-Tallaa, L., et al., 2013. The carcinogenicity of outdoor air pollution. Lancet Oncol. 14, 1262.

McDonald, J.D., Zielinska, B., Fujita, E.M., Sagebiel, J.C., Chow, J.C., Watson, J.G., 2000. Fine particle and gaseous emission rates from residential wood combustion. Environ. Sci. Technol. 34, 2080–2091.

McGarry, P., Morawska, L., He, C., Jayaratne, R., Falk, M., Tran, Q., et al., 2011. Exposure to particles from laser printers operating within office workplaces. Environ. Sci. Technol. 45, 6444–6452.

Nimmrichter, J., Kautek, W., Schreiner, M., 2007. Lasers in the Conservation of Artworks. Springer.

OSHA (Occupational Safety and Health Administration), 1998. Permissible Exposure Limits-Annotated Tables, Available: https://www.osha.gov/dsg/annotated-pels/. Accessed September 28, 2020.

OSHA (Occupational Safety and Health Administration), 1993. Regulations (Standards – 29 CFR), Available: https://www.osha.gov/laws-regs/regulations/standardnumber/1910. Accessed September 28, 2020.

Pashby, I., Barnes, S., Bryden, B., 2003. Surface hardening of steel using a high power diode laser. J. Mater. Process. Technol. 139, 585–588.

Thorley, A.J., Ruenraroengsak, P., Potter, T.E., Tetley, T.D., 2014. Critical determinants of uptake and translocation of nanoparticles by the human pulmonary alveolar epithelium. ACS Nano 8, 11778–11789.

Ullmann, M., Friedlander, S.K., Schmidt-Ott, A., 2002. Nanoparticle formation by laser ablation. J. Nanoparticle Res. 4, 499–509.

USEPA (United States Environmental Protection Agency), 2017. Partilce Pollution Exposure, Availale: https://www.epa.gov/pmcourse/particle-pollution-exposure. Accessed September 28, 2020.

USEPA (United States Environmental Protection Agency), 2020. IRIS Assessments, Available: https://cfpub.epa.gov/ncea/iris_drafts/atoz.cfm. Accessed September 28, 2020.

Vassie, L., Roach, R., Tyrer, J.R., Sharp, B., 1995. Fumes generated during laser processing of polyvinyl chloride (PVC). Opt. Laser Technol. 27, 31–37.

Walter, J., Hustedt, M., Staehr, R., Kaierle, S., Jaeschke, P., Suttmann, O, et al., 2014. Laser cutting of carbon fiber reinforced plastics–investigation of hazardous process emissions. Phys. Procedia 56, 1153–1164.

Zhang, S., Wang, X., He, M., Jiang, Y., Zhang, B., Hang, W., et al., 2014. Laser-induced plasma temperature. Spectrochim. Acta B 97, 13–33.